DOI: 10.1002/chem.200500690

Isocytosine as a Hydrogen-Bonding Partner and as a Ligand in Metal Complexes

Deepali Gupta, Michael Roitzsch, and Bernhard Lippert*[a]

Abstract: Isocytosine (ICH; **1**) exists in solution in an equilibrium of tautomers **1a** and **1b** with the N^1 and N^3 positions carrying the acidic proton, respectively. In the solid state, both tautomers coexist in a 1:1 ratio. As we show, the N^3H tautomer **1b** can selectively be crystallized in the presence of the model nucleobase 1-methylcytosine (1-MeC). The complex **1b**·(1-MeC)·2H_2O (**2**) forms pairs through three hydrogen bonds between the components; hydrogen bonds between identical molecules are also formed, leading to an infinite tape structure. On the other hand, the N^1H tautomer **1a** co-crystallizes with protonated ICH to give [**1a**·ICH_2]NO_3 (**3**), again with three hydrogen bonds between the partners, yet the acidic proton is disordered over the two entities. With M^{II}(dien) (M = Pt, Pd; dien = diethylenetriamine) preferential coordination of tautomer **1a** through the N3 position is observed. DFT calculations, which were also extended to Pt^{II}(tmeda) linkage isomers (tmeda = *N*,*N*,*N*′,*N*′-tetramethylethylenediamine), suggest that intramolecular hydrogen bonding between the ICH tautomers and the co-ligands at M, while adding to the preference for N^3 coordination, is not the major determining factor. Rather it is the inherently stronger Pt–N^3 bond which favors complexation of **1a**. With an excess of M^{II}(dien), dinuclear species $[M_2(dien)_2(IC\text{-}N^1,N^3)]^{3+}$ (M = Pd^{II}, **4** and Pt^{II}, **5**) also form and were isolated as their ClO_4^- salts and structurally characterized. In strongly acidic medium **5** is converted to $[Pt(dien)(ICH\text{-}N^1)]^{2+}$ (**6**), that is, to the Pt^{II} complex of tautomer **1b**.

Keywords: hydrogen bonding · isocytosine · palladium · platinum · tautomerism

Introduction

Isocytosine (ICH, 2-aminopyrimidin-4-(3*H*)-one) is an isomer of the natural parent nucleobase cytosine. ICH exists as two major tautomers, **1a** and **1b**,[1] which crystallize in a 1:1 ratio and form a hydrogen-bonded adduct[2] in the solid state (Scheme 1). The N^1[3,4] and C^5-glycosidic[5] derivatives of ICH are of certain interest in pharmacology and molecular biology. As pointed out by us in a previous paper,[6] our particular interest in this ligand was the metal binding behavior of tautomer **1b** and specifically the attachment of a Pt^{II} entity to the N^1 position. This way we had hoped to generate platinated nucleobase analogues (Scheme 2) which, when incorporated into a suitable backbone,[7] might give rise to artificial, cationic oligonucleotide analogues with the ability to recognize natural nucleobases through hydrogen-bond formation. As it turned out, tautomer **1a** is more reactive toward metal ions, leading to preferential binding of Pt^{II} and Pd^{II} electrophiles through the N^3 position.

Here, we report on our continuing efforts of reaching the goal of N^1 metal coordination. At the same time, we have examined the possibility of shifting the equilibrium between

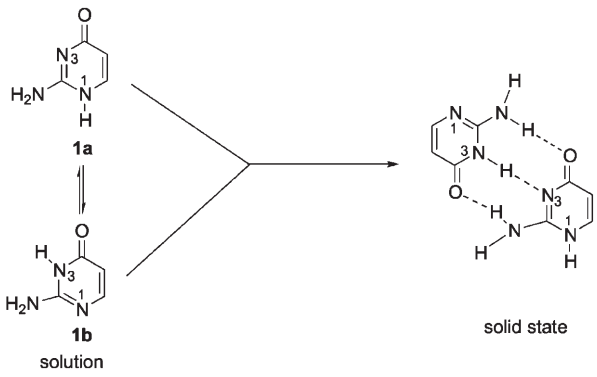

Scheme 1. Tautomerism of isocytosine in solution (**1a**, **1b**) and hydrogen-bonded adduct **1a**·**1b** in the solid state.

[a] D. Gupta, M. Roitzsch, Prof. Dr. B. Lippert
Fachbereich Chemie, Universität Dortmund
Otto-Hahn-Str. 6, 44221 Dortmund (Germany)
Fax: (+49) 231-755-3797
E-mail: bernhard.lippert@uni-dortmund.de

Supporting information for this article is available on the WWW under http://www.chemeurj.org/ or from the author.

 © 2005 Wiley-VCH Verlag GmbH & Co. KGaA, Weinheim

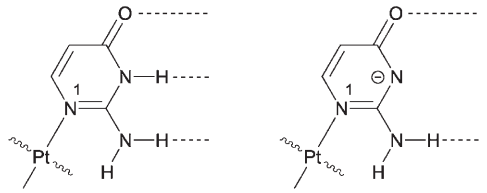

Scheme 2. N^1-platinated forms of isocytosine (neutral ligand left; anionic ligand right).

1a and **1b** by adding a co-hydrogen-bonding partner that exclusively interacts with one of the two tautomers. This aspect relates to the more general and in particular biologically relevant question of nucleobase tautomerism and mispairing leading to mutagenesis.

Results and Discussion

Influence of hydrogen-bonding partners on tautomer equilibrium of ICH: A number of temperature-dependent solution studies[8] have been carried out that suggest that ICH exists in solution as a mixture of the two forms **1a** and **1b**. However, these studies were not able to distinguish which tautomer predominates. It has also been observed that the electronic absorption spectra[8–13] of ICH change on going from aqueous to nonaqueous solution. Therefore, it was postulated that this behavior of ICH might be dependent on the change of tautomeric ratio caused by the nature of solvent and the temperature; ICH exists predominately in the keto-N^3H form **1b** in ethanol and diethyl ether, while in aqueous solution the two tautomers **1a** and **1b** coexist in comparable amounts.

We have previously reported[6] that certain bands in the Raman spectra of ICH also shift to higher wavenumbers, that is, from 789 to 791 cm^{-1} and from 1214 to 1232 cm^{-1}, as DMF is successively diluted with water, though there was no separation into individual peaks as is the case for isocytosine in the solid state and in pure DMF.

In a similar way it has been demonstrated that 2′-deoxy-N^6-methoxyadenosine (mo^{6}A) can undergo amino–imino tautomerism, depending on the hydrogen-bonding partner added,[14,15] and detection of createnine by a designed receptor is accompanied by a change in tautomer structure of the receptor.[16] In more general terms, it is evident that tautomer equilibria are subject to changes in the presence of components capable of interacting with one of the two tautomers preferentially.[17] Therefore, we were intrigued by the possibility of shifting the equilibrium between **1a** and **1b** by adding a co-hydrogen-bonding partner that exclusively interacts with one of the two tautomers.

As pointed out in the introduction (Scheme 1), crystallization of ICH from water yields a 1:1 distribution of the two tautomers **1a** and **1b**, which is favorable as a consequence of complementary hydrogen bonding between the two tautomers. Co-crystallization of ICH with 1-methylcytosine (1-MeC) from H_2O gave crystals of **1b**·(1-MeC)·2H_2O (**2**). A

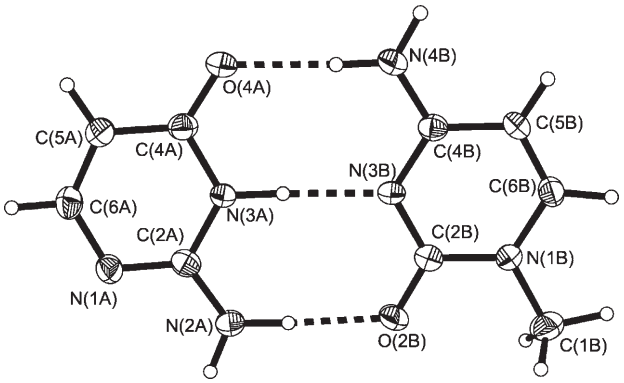

Figure 1. View of the hydrogen-bonded pair ICH·(1-MeC)·2H_2O (**2**). ICH is present as tautomer **1b**. The water molecules are omitted for clarity.

view of the hydrogen-bonded pair is given in Figure 1. The two different heterocycles are readily distinguished due to the presence of a methyl group in 1-MeC. In the solid, the 1:1 triply hydrogen-bonded complex consists of neutral 1-MeC and ICH bases, bonded in a Watson–Crick fashion. ICH is present exclusively as its keto-N^3H tautomer **1b**. In addition to the unambiguous location and refinement of the proton at N^3 of ICH, the heavy atom geometrical parameters are in accord with this interpretation. The exclusive presence of **1b** is also firmly established by the large value of the endocyclic bond angle at N^3, C(2A)-N(3A)-C(4A), 122.1(2)°. The bond-length changes are minimal for 1-MeC[18] and ICH.[1] Structural details of the two heterocycles are listed in Table 1.

Table 1. Selected bond lengths [Å] and angles [°] for **2**.

	ICH	1-MeC
O(4)–C(4)	1.255(3)	–
O(2)–C(2)	–	1.248(3)
N(1)–C(2)	1.345(2)	1.395(3)
N(1)–C(6)	1.355(3)	1.365(3)
N(3)–C(2)	1.369(3)	1.352(3)
N(3)–C(4)	1.379(3)	1.340(2)
N(4)–C(4)	–	1.332(3)
C(5)–C(6)	1.351(3)	1.416(3)
N(1)-C(2)-N(3)	122.8(2)	119.2(2)
N(1)-C(6)-C(5)	126.3(2)	121.3(2)
C(2)-N(1)-C(6)	120.9(2)	120.4(2)
C(2)-N(3)-C(4)	122.1(2)	119.6(2)
N(2)-C(2)-N(3)	116.7(2)	–
O(2)-C(2)-N(3)	–	122.3(2)
N(3)-C(4)-C(5)	115.5(2)	116.7(2)

The isocytosine moiety and 1-MeC are nearly coplanar (deviation 3.6°). The interbase hydrogen bonding is strong and nearly linear, namely, N(4B)–H···O(4A) = 1.94(2), N(3A)–H···N(3B) = 1.861(2), and N(2A)–H···O(2B) = 1.85(2) Å, corresponding to distances of 2.882(3), 2.894(3), and 2.874(3) Å between the heavy atoms. In addition to this principal hydrogen-bonding pattern, pairs of **1b** and 1-MeC

 © 2005 Wiley-VCH Verlag GmbH & Co. KGaA, Weinheim

are further linked by hydrogen bonds between N(4B)···O-(2BA) (2.893(3) Å) and N(2A)···O(4AB) (2.904(3) Å) to produce a tape structure (Figure 2). These hydrogen bonds

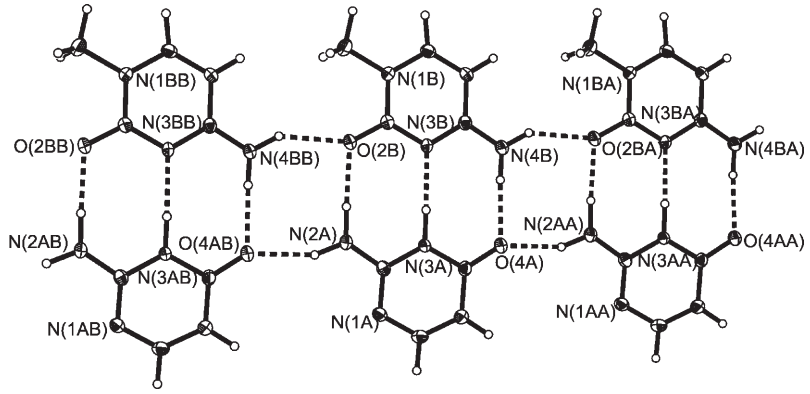

Figure 2. Pairs within **2** associate by means of additional hydrogen bonds to give an infinite tape structure. The water molecules are omitted for clarity.

are between identical molecules; hence, contacts are between 1-MeC molecules on one hand and **1b** molecules on the other. Tapes of **2** extend along the *b* axis, with mean stacking distances of 3.50 Å and opposite directions between stacked tapes. Additional hydrogen bonding involving the water of crystallization also contributes to the overall crystal stability: O(2W)–H···O(4A) = 2.996(3) and O(1W)–H···N(1A) = 2.909(3) Å. In addition, there is a weak contact between C(6B)–H and O(1W) at 3.623(3) Å.

A Raman spectrum of **2** was recorded in the solid state in the spectral range 400–1700 cm^{-1}. There are characteristic bands present at 774 and 782 cm^{-1} as well as at 1264 and 1217 cm^{-1}, due to complex ring bending and stretching modes of 1-MeC and ICH. A comparison of Raman spectra of 1-MeC,[19] ICH,[6] and compound **2** suggests that the band at 774 cm^{-1} is due to the ring deformation mode of 1-MeC, while the band at 782 cm^{-1} is assigned a similar mode of the keto-N^3H tautomer **1b** of isocytosine. Similarly, the band at 1264 cm^{-1} is assigned to the stretching mode of 1-MeC and, correspondingly, the other band at 1217 cm^{-1} to the keto-N^3H tautomer **1b**.

Although it is possible to postulate complementary hydrogen-bond formation between the ICH tautomer **1a** and a guanine nucleobase (Scheme 3), we were unable to prove such a possibility. Attempts to co-crystallize ICH and 9-methylguanine or guanosine did not yield 1:1 adducts, possibly due to the low solubilities of the guanine components relative to ICH in water. However, even ^{1}H NMR spectroscopy in [D_6]DMSO did not provide any compelling evidence in favor of such a hydrogen-bonding pattern. Although a concentration dependence of 1:1 mixtures of ICH and guanosine could be obtained, albeit in a narrow concentration range only (10–70 mMol L^{-1}), the downfield shift of NH and NH_2 resonances with increasing concentrations were within the range found for self-association of the individual components guanosine[20] and ICH (data not shown), hence in the order of $\delta = 0.03$ ppm for the concentration range mentioned. These ^{1}H NMR studies were hampered by the fact that the DMSO samples were not free of water and contained between 2.5 and 5 equiv of H_2O per guanosine and ICH, with more diluted samples having a higher water content. Addition of molecular sieves, while reducing the water content and increasing the downfield shifts of the NH_2 resonances clearly beyond those of self-pairing, at the same time led to coalescence of the two NH protons (broad resonance at $\delta =$ 10.82 ppm, halfwidth ca. 180 Hz) due to exchange. We have observed this phenomenon before and believe that it is due to the partial hydrolysis of the zeolite and generation of OH^-.

Eventually, the goal of selectively crystallizing the keto-N^1H tautomer **1a** was achieved in the presence of protonat-

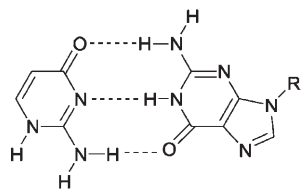

Scheme 3. Feasible hydrogen-bond formation between the Watson–Crick face of guanine and the O(4)-N(3)-N(2) face of tautomer **1a** of ICH.

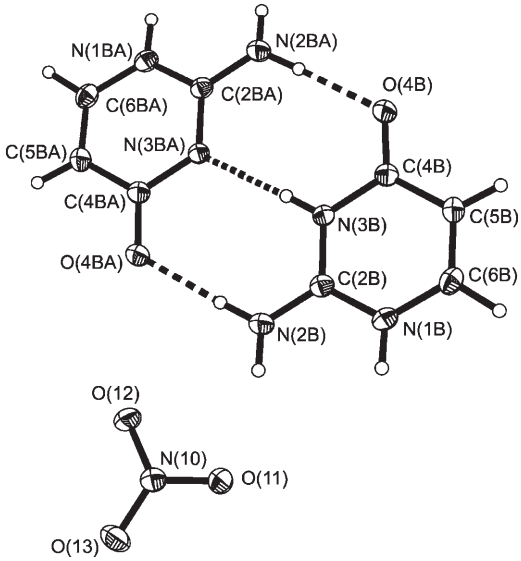

Figure 3. View of one (II) of the two crystallographically independent hydrogen-bonded pairs present in [**1a**·ICH_2]NO_3 (**3**). Only one position of the disordered proton in the central hydrogen bond is shown.

 © 2005 Wiley-VCH Verlag GmbH & Co. KGaA, Weinheim

ed isocytosine. The complex $[\mathbf{1a}\cdot ICH_2]NO_3$ (**3**) was isolated as single crystals and studied by X-ray analysis. The structure of **3** consists of two crystallographically independent entities (I, II) and two nitrate anions. Both heterocycles form pairs with their own symmetry related moieties. This feature is reminiscent of that of $[C\cdot CH]_2[ZnCl_4]$ (C = unsubstituted cytosine, CH = cytosinium), in which two independent, hydrogen-bonded base pairs between cytosinium and cytosine are formed.[21] Each pair is held together by three hydrogen bonds between the respective O^2, N^3, and N^4 sites (Figure 3). The central proton, that between the two N^3 sites, is disordered over two positions, both of which have been detected in the electron density map. The large values of the endocyclic bond angles at N3(A/B) (C2(A/B)-N3(A/B)-C4(A/B), ca. 122° and N1(A/B), C2(A/B)-N1(A/B)-C6-(A/B), ca. 121°) also indicate that the proton is disordered over the central hydrogen bond. Within the two pairs, the two isocytosine rings cannot be differentiated into neutral and protonated form, and the geometries of the two rings are identical within standard deviations (Table 2). Thus, the situation is different from that for neutral isocytosine,[1] in which the two tautomers **1a** and **1b** are clearly identified on the basis of significant differences in a number of bond lengths and internal ring angles. Despite this disorder, there can be no doubt, however, that **3** represents the adduct between tautomer **1a** and the isocytosinium ion (ICH_2^+). Regardless where the central proton is located, it will always generate a pair of **1a** and ICH_2^+ (Scheme 4).

Table 2. Selected bond lengths [Å] and angles [°] for **3**.

	3		**ICH**[1]	
	A[a]	B[a]	**1a**	**1b**
O(4)−C(4)	1.237(2)	1.250(2)	1.248(3)	1.246(3)
N(1)−C(6)	1.363(3)	1.358(3)	1.358(3)	1.350(3)
N(1)−C(2)	1.345(2)	1.354(3)	1.357(3)	1.330(3)
N(2)−C(2)	1.314(3)	1.310(3)	1.323(3)	1.324(3)
N(3)−C(2)	1.342(3)	1.338(2)	1.333(3)	1.369(3)
N(3)−C(4)	1.381(2)	1.374(3)	1.363(3)	1.375(3)
C(4)−C(5)	1.437(3)	1.433(3)	1.438(3)	1.422(3)
C(5)−C(6)	1.330(3)	1.333(3)	1.331(3)	1.356(3)
N(1)-C(2)-N(3)	119.7(2)	119.5(2)	121.8(1)	121.9(1)
N(1)-C(2)-N(2)	120.7(2)	119.9(2)	118.9(1)	120.3(1)
N(1)-C(6)-C(5)	121.2(2)	120.9(2)	120.5(1)	125.9(1)
C(2)-N(1)-C(6)	120.9(2)	121.1(2)	120.2(1)	115.9(1)
C(2)-N(3)-C(4)	122.1(2)	121.9(2)	119.4(1)	123.3(1)
N(2)-C(2)-N(3)	119.6(2)	120.6(2)	119.3(1)	117.8(1)
O(4)-C(4)-C(5)	123.5(2)	123.1(2)	122.0(1)	126.4(1)
O(4)-C(4)-N(3)	119.8(2)	119.6(2)	119.3(1)	118.8(1)
N(3)-C(4)-C(5)	116.7(2)	117.3(2)	118.7(1)	114.8(1)
C(4)-C(5)-C(6)	119.3(2)	119.3(2)	119.1(1)	118.2(1)

[a] Molecules A and B in hemiprotonated ICH.

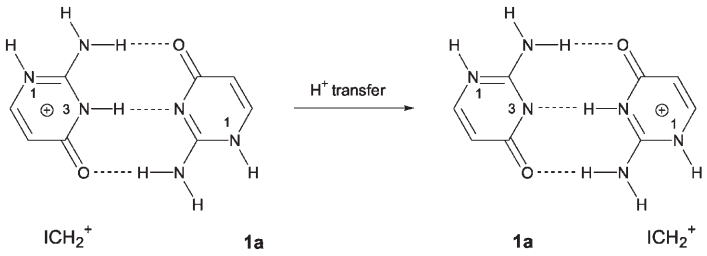

Scheme 4. Hydrogen-bonded adduct of **1a** and ICH_2^+ as present in compound **3**. H^+ transfer does not alter the composition.

Hydrogen-bonding distances within the two crystallographically different pairs are N(3A)···N(3AB) = 2.842(2) and N(3B)···N(3BA) = 2.835(2) Å, for I and II respectively, and N(2A)···O(4AB) = 2.834(2) and N(2B)···O(4BA) = 3.022(3) Å, also for I and II, respectively. In hemiprotonated 1-methylcytosine compounds $([(1\text{-MeC})_2H]^+X^-)$[22] the length of the central hydrogen bond compares well with that found in **3**, but the outer hydrogen bonds (ca. 2.75 vs 2.90 Å) differ markedly, as expected. The same should be expected for **3** in the absence of disorder.

Pairs I and II of $\mathbf{1a}\cdot ICH_2^+$ are part of a ribbon structure which forms as a consequence of additional hydrogen bonds between pairs I and II (Figure 3). Of pair I, $N(2)H_2$ groups act as donors and O(4) sites as acceptors, whereas of pair II, C(5)H sites act as donors and O(4) sites as acceptors. The four intermolecular hydrogen bonds between pairs I and II are then between O(4A) (I) and C(5BA)H (II), 3.196(3) Å as well as $N(2AB)H_2$ (I) and O(4BA) (II), 3.022(3) Å. The hydrogen bond between C(5)H and O(4) is reminiscent of similar hydrogen bonds found in recent years between nucleobases.[23]

As can be also seen from Figure 4, the nitrate anions of **3** are involved in hydrogen bonding as well. The shortest ones are those that involve N^1H (N···O = 2.77(3)–2.80(2) Å) or

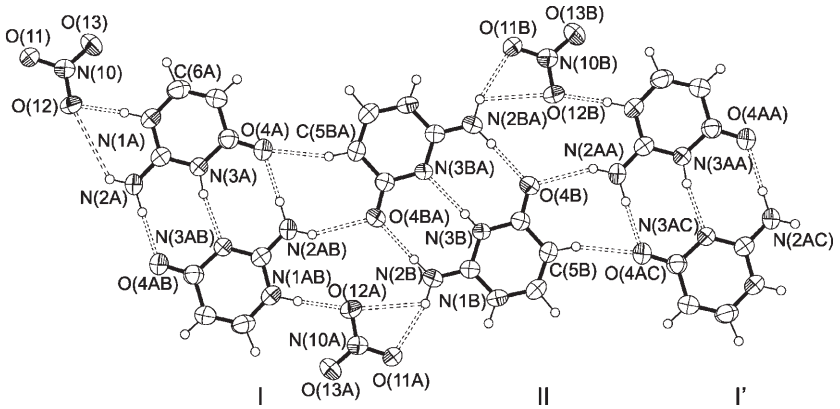

Figure 4. Association of the crystallographically independent pairs of I and II and the nitrate anions in **3**. In both pairs of **1a** and ICH_2^+ disordered protons have been fixed in the idealized positions in the central hydrogen bonds.

 © 2005 Wiley-VCH Verlag GmbH & Co. KGaA, Weinheim

NH_2 (N···O = 2.99(3) Å) sites. Pairs of I and II, as well NO_3^-, form a tape structure with individual tapes forming stacks with stacking distances of approximately 3.3 Å. There are additional weak short contacts between the nitrate oxygen atoms and aromatic hydrogen atoms, that is, C^5H···O = 3.507(3) Å and C^6H···O = 3.507(3) Å.

Metal complexes of ICH: We have previously reported the crystal structure of $[Pd(dien)(ICH\text{-}N^3)](NO_3)_2$,[6] and now present the preparation and structural characterization of dimetalated species $[M_2(dien)_2(IC\text{-}N^1,N^3)](ClO_4)_3$ (M = Pd^{II}, **4** and Pt^{II}, **5**). Mixtures of isocytosine and $[M(dien)(D_2O)]^{2+}$ (1:3) were kept at 40 °C for a few hours. Initially, a typical spectrum at pD 4.6 consisted of four sets of aromatic C^5H and C^6H isocytosine resonances (doublets each, $^3J \sim$ 6.7–7.3 Hz). The most intense set of resonances was due to the N^3 linkage isomer and, correspondingly, the other sets of resonances belonged to the free ligand, the N^1 linkage isomer, and the N^1,N^3 dinuclear species.[6] The pD's of the samples were subsequently adjusted to 7.6 and solutions of $[M(dien)(D_2O)]^{2+}$ in D_2O were successively added to the reaction mixtures. This was repeated until only a single set of resonances due to **4** or **5** was observed. Both **4** and **5** display ^{1}H NMR resonances that are insensitive to pD over a wide range. However, at pD 1.2, complex **4** decomposes to give ICH and Pd^{II}(dien), whereas **5** is converted into **6** (see below).

A view of the molecular cation **4** is shown as a representative example in Figure 5. The molecular structure of **5** was found to be very similar (Supporting Information). Selected bond lengths and angles for **4** and **5** are given in Table 3. Pd and Pt have the expected square-planar coordination geometries. As can be seen, metals are bonded through N^1 and N^3 positions of the IC; M(1)–N^1 bond has the distances ranging from 2.026(6) to 2.034(3) Å and the M(2)–N^3 bond from 2.037(3) to 2.039(6) Å for Pd and Pt, respectively. Distances and angles within the IC ligand are not unusual. Angles about Pd and Pt deviate markedly from ideal square-planar geometry(e.g., N(1a)-M(1)-N(2a), 84.6(2) and 84.9(2)°; N(1a)-M(1)-N(3a), 167.8(2) and 176.6(2)°; N(1b)-M(2)-N(2b), 84.9(2) and 85.2(2)°; N(1b)-M(2)-N(3b), 168.4(2) and 169.1(3)° for Pd and Pt, respectively). The M–N(dien) distances range from 1.999(4) Å in M(1)–N(2a) or M(2)-N(2b) to 2.039(4) Å in M(1)-N(3a) or M(2)-N(3b), and are likewise normal. The dien ligands, "a" and "b", adopt the characteristic sting-ray geometries[24] with the central methylene groups C(2) and C(3) of the two dien ligands pointing in the same direction, yet in opposite directions for "a" and "b". Deviations of carbon atoms of the two dien ligands from the least-squares planes formed by the PtN_4 planes are −0.52(1) (C2a), −0.36(1) (C3a), −0.02(1) (C1a), 0.29(1) (C4a) and 0.50(1) (C2b), 0.62(1) (C3b), −0.003(1) (C4b), −0.15(1) Å (C1b). Thus, the two halves of the dien ligands undergo marked distortions from the case of a symmetrical distribution of the two carbon atoms of an ethylenediamine ring.[25] For the corresponding Pd compound, these values are rather similar. The IC planes form angles of approximately 86° and 74° with the respective Pd(1)/Pt(1) and Pd(2)/Pt(2) coordination planes. The external angles at N^1 and N^3 (M(1)-N(1)-C(6), 120–121°; M(1)-N(1)-C(2), 120–122°; M(2)-N(3)-C(4), 118–119°; M(2)-N(3)-C(2), 120–121°) are quite similar. The water molecules, dien ligands, perchlorate anions, $N(2)H_2$ and O(4) of the IC ligand are involved in numerous intramolecular and intermolecular short contacts. For example, the protons at N(1a/b), N(2a/b), and N(3a/b) of dien ligands are hydrogen bonded to various oxygen atoms of different perchlorate anions, water molecules and O(4) of the IC ligand, whereas the two protons of N(2) in IC form hydrogen bonds to oxygen of a perchlorate anion and a water molecule. A

Table 3. Selected bond lengths [Å] and angles [°] for **4**, **5**.

	4	**5**
M(1)···M(2)	5.90(2)	5.89(2)
$M(1)N_4$/ICH[a]	86.9(1)	86.2(2)
$M(2)N_4$/ICH[a]	74.6(1)	74.8(2)
M(1)–N(1)	2.034(3)	2.026 (6)
M(1)–N(1a)	2.042(3)	2.039(5)
M(1)–N(2a)	1.999(3)	2.006(8)
M(1)–N(3a)	2.034(3)	2.033(5)
M(2)–N(3)	2.037(3)	2.039(6)
M(2)–N(1b)	2.032(3)	2.037(5)
M(2)–N(2b)	1.999(4)	2.009(8)
M(2)–N(3b)	2.048(3)	2.049(5)
C(2)-N(1)-C(6)	116.6(4)	116.1(6)
C(2)-N(3)-C(4)	120.3(4)	120.6(6)
N(1)-C(2)-N(3)	123.9(3)	124.0(4)

[a] Dihedral angle between metal coordination plane (MN_4) and ICH.

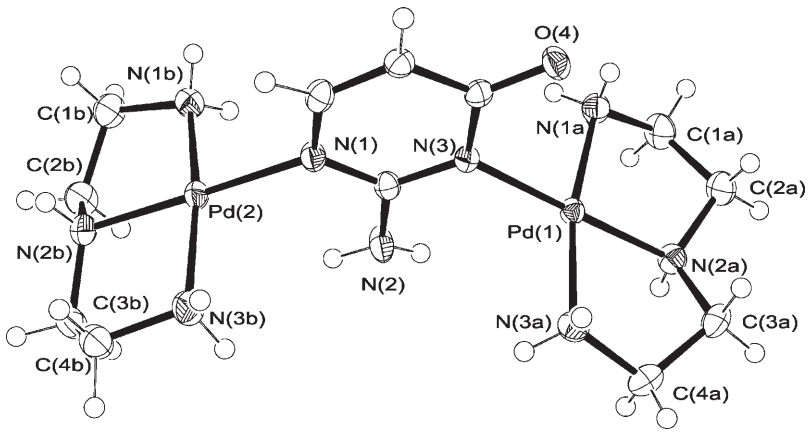

Figure 5. View of cation of $[Pd_2(dien)_2(IC\text{-}N^1,N^3)](ClO_4)_3$ (**4**) with atom numbering scheme. The cation of the corresponding Pt compound **5** is rather similar and is not shown.

 © 2005 Wiley-VCH Verlag GmbH & Co. KGaA, Weinheim

motif is also present in the solid structure in which O(4) of the IC ligand hydrogen bonds to protons at N(1) of dien ligands of two different molecules. None of these contacts (2.9–3.1 Å) between heavy atoms is particularly short.

In the course of the ^{1}H NMR spectroscopic studies, it was noticed that in acidic medium the dinuclear complex **5** could be converted into the mononuclear complex [Pt(dien)(ICH-N^1)]$^{2+}$ (**6**), which contains the desired tautomer **1b** bonded to Pt through the N^1 position. Unfortunately, our attempts to isolate **6** have failed so far. We propose that removal of the Pt^{II}(dien) entity from N^3 of **5** follows a route that we have previously shown to take place with N^3-platinated 1-methyluracil and 1-methylthymine model nucleobases.[26] According to it, protonation of the exocyclic O(4) oxygen atom labilizes the Pt–N^3 bond to such an extent that it breaks (Scheme 5). The enol tautomer formed initially converts then quickly into the oxo tautomer **6**.

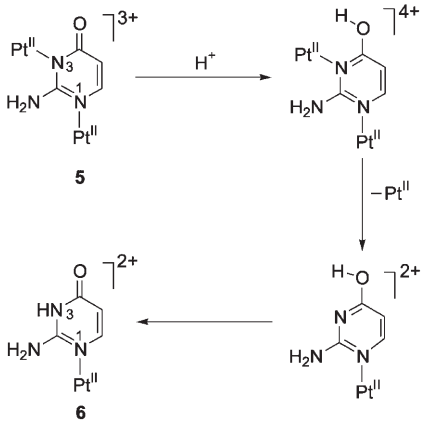

Scheme 5. Proposed removal of the Pt^{II}(dien) entity from N^3 of **5**.

Theoretical calculations: Molecular geometries of a series of compounds have been computed in order to better understand the apparent preference of Pt^{II} and Pd^{II} electrophiles for the N^3 site of ICH. Figure 6 provides views of optimized structures of [Pd(dien)(ICH-N^1)]$^{2+}$, [Pd(dien)(ICH-N^3)]$^{2+}$, [Pt(dien)(ICH-N^1)]$^{2+}$, [Pt(dien)(ICH-N^3)]$^{2+}$, [Pt(tmeda)-(ICH-N^1)]$^{2+}$, and [Pt(tmeda)(ICH-N^3)]$^{2+}$. Calculations were also performed on dinuclear complexes of M^{II}(dien), namely, [Pd$_2$(dien)$_2$(IC-N^1,N^3)]$^{3+}$ and [Pt$_2$(dien)$_2$(IC-N^1,N^3)]$^{3+}$. The structures of these last two complexes were found to be very similar. The optimized structure of [Pt$_2$-(dien)$_2$(IC-N^1,N^3)]$^{3+}$ is depicted in Figure 7 as a representative example.

The N^1 linkage isomers of M(dien) (M = Pd^{II}, Pt^{II}) are similar. The angle between the MN$_4$ plane and the ICH plane is 64.2° (M = Pd) and 69.0° (M = Pt). It is possible only as a result of the intramolecular hydrogen bond, which is between the exocyclic amino group N(2)H$_2$ of ICH and one of the two amino groups of the dien ligand. As can be seen, the ICH amino group has undergone some pyramidalization to be able to act as a hydrogen bond acceptor, but the hydrogen bond (N(2)H$_2$–NH$_2$(dien) 3.287 Å for Pd and

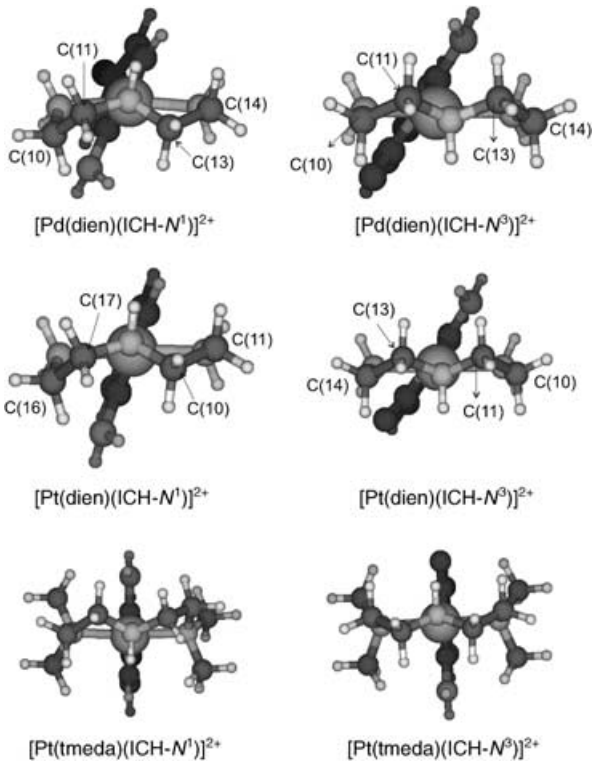

Figure 6. Optimized computed structures of [Pd(dien)(ICH-N^1)]$^{2+}$, [Pd-(dien)(ICH-N^3)]$^{2+}$, [Pt(dien)(ICH-N^1)]$^{2+}$, [Pt(dien)(ICH-N^3)]$^{2+}$, [Pt-(tmeda)(ICH-N^1)]$^{2+}$, and [Pt(tmeda)(ICH-N^3)]$^{2+}$.

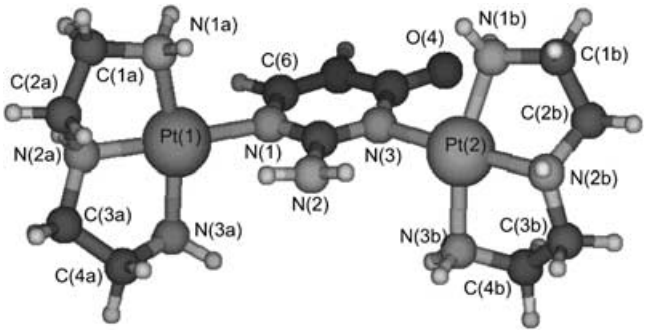

Figure 7. Optimized structure of [Pt$_2$(dien)$_2$(IC-N^1,N^3)]$^{3+}$ with atom numbering scheme. The structure of the corresponding Pd compound is rather similar and is not shown.

3.425 Å for Pt compound) is not to be considered particularly strong, owing to a somewhat unfavorable angle between the dien-NH$_2$ donor and the acceptor. Nevertheless, this hydrogen bond appears to be responsible for the differences in distortions of the two "en" halves of the dien ligands. Deviations of carbon atoms from the mean-squares planes in the Pd complex are −0.89 (C10) and −0.25 Å (C11), as opposed to −0.69 (C13) and −0.15 Å (C14). For the corresponding Pt compound, these values are rather similar.

The N^3 linkage isomers of M^{II}(dien) are likewise very similar. The ICH plane is tilted by 58.5° (Pd) and 56.0° (Pt), respectively, relative to the MN$_4$ coordination plane. Both

 © 2005 Wiley-VCH Verlag GmbH & Co. KGaA, Weinheim

NH_2 groups of the dien ligands are involved in hydrogen-bond formation with O(4) as well as $N(2)H_2$ of ICH. The hydrogen-bond lengths are 2.843 and 2.826 Å for O(4)···NH_2(dien) in the Pd and Pt complexes, respectively, whereas those involving the $N(2)H_2$ of ICH and dien-NH_2 are 3.435 Å (Pd) and 3.336 Å (Pt). Again, the exocyclic NH_2 group of ICH has undergone a marked pyramidalization. The dien puckers have the characteristic sting-ray geometries[25] with the central methylene groups C(2) and C(3) above the MN_4 plane. Deviations of carbon atoms from the mean-squares planes for the Pd complex are −0.11 (C10) and 0.52 Å (C11), as opposed to 0.53 (C13) and −0.06 Å (C14). These deviations are comparable to those of the Pt complex.

A comparison of the total energies of the ICH linkage isomers of M^{II}(dien) reveals that both for Pd and Pt the N^3 isomers are lower in energy, by 15.97 kcal mol^{-1} (Pd) and 15.87 kcal mol^{-1} (Pt). These energy differences are larger than those found for the isomeric complexes of $Pt^{II}(NH_3)_3$, in which the N^3 site was preferred by $\Delta E = 12.2$ kcal mol^{-1}. The N^3 isomer of $Pt^{II}(NH_3)_3$ adopts a similar orientation (dihedral angle 55°) as seen in [Pt(dien)(ICH-N^3)]$^{2+}$, with a normal hydrogen bond of 2.79 Å between NH_3 of Pt and O(4) of ICH, and a long contact (3.27 Å) between NH_3 of Pt and $N(2)H_2$ of ICH. In contrast, in [$Pt(NH_3)_3$(ICH-N^1)]$^{2+}$ the ICH ligand is perpendicular to the PtN_4 plane with no hydrogen-bonding interactions between ICH and the two *trans*-positioned NH_3 ligands at all, unlike in [Pt(dien)(ICH-N^1)]$^{2+}$ (see above). We conclude from this difference that the hydrogen bond between ICH-$N(2)H_2$ and the dien-NH_2 group must be very weak and that the preference for N^3 is aided by formation of the hydrogen bond involving O(4) of the N^3 linkage isomer.

As expected the calculated structures of the ICH linkage isomers of *N*,*N*,*N*′,*N*′-tetramethylethylenediamineplatinum(II) (Pt^{II}tmeda), reveal that in neither isomer is there an involvement of any of the exocyclic groups of the ICH in intramolecular hydrogen bonding. The dihedral angles between the ICH and the PtN_4 planes are 89.6° and 90.0° for N^1 and N^3 linkage isomers, respectively. Moreover, and consistent with this view, is the planarity of $N(2)H_2$ group. The puckers of the two halves of the tmeda ligand are nevertheless somewhat distorted (see the Supporting Information). The energy difference between the two isomers is 11.56 kcal mol^{-1} in favor of the N^3 isomer. A comparison of all the three systems, that is, of $Pt^{II}(NH_3)_3$, Pt^{II}(dien), and Pt^{II}(tmeda) therefore suggests that the higher strength of the Pt−(ICH-N^3) bond is the major determinating factor in the preference for binding, and that intramolecular hydrogen bonding involving O(4) in the N^3 isomer adds to the stability, while the contribution of $N(2)H_2$ group to hydrogen bonding is small.

Finally, the structures of the dinuclear complexes [M_2(dien)$_2$(IC-N^1,N^3)]$^{3+}$ (M = Pd^{II} and Pt^{II}) have been calculated. There is generally good agreement between the calculated dinuclear compounds of Pd^{II}(dien) and Pt^{II}(dien) and the X-ray structures of **4** and **5**, respectively. Discrepancies are probably a consequence of crystal packing forces and the presence of the counterions in the solid-state structures. For instance, in the calculated complex, the angle between the $Pd(1)N_4$ plane and the IC plane is 62.3°, yet this angle is 86.9° in the solid-state structure (see Table 3). Similarly, the angle between the $Pt(2)N_4$ plane and the IC plane is 63.3°, which is much smaller than that found in the X-ray structure. The angle between the $Pd(2)N_4$ plane and the IC plane is 70.6° and the angle between the $Pt(1)N_4$ plane and the IC plane is 82.7°; these values are in the same range as those found in the X-ray-characterized complexes **4** and **5**, respectively. The M−N(dien) distances range from 2.07 Å in M(1)−N(2A) or M(2)−N(2B) to 2.122 Å in M(2)−N(3A) or M(2)−N(3B), and are likewise normal. For Pd and Pt complexes, the dien ligands (A and B) bonded to N^1 and N^3 positions of IC have different geometries. Deviations of carbon atoms of the dien ligand from the mean-squares planes formed by the $M(1)N_4$ plane range from −0.11 to −0.30 Å (C1a), −0.65 to −1.04 Å (C2a), −0.24 to −0.80 Å (C3a), and −0.89 to −1.41 Å (C4a) and for $M(2)N_4$ plane range from 0.30 Å (C1b), 0.81 to 0.87 Å (C2b), 0.34 to 0.39 Å (C3b), and 0.95 to 1.0 Å (C4b). The angles and bond lengths of the IC ring are normal. The NH_2 groups of the dien ligands are involved in hydrogen-bond formation with O(4). The hydrogen-bond lengths are 2.871 Å (Pd) and 2.806 Å (Pt) for O(4)···NH_2(dien). Only in the case of the Pd complex is there a short contact between $N(2)H_2$ of IC and (dien)-NH_2 (3.341 Å). Again, the exocyclic NH_2 group of IC has undergone a slight pyramidalization.

Discussion

External factors are known to affect tautomer equilibria. Apart from factors such as aggregation state, solvent, and temperature, the presence of hydrogen-bonding partners or metal coordination can shift tautomer equilibria.[14–17] Here, we have demonstrated that the two dominant tautomers of isocytosine, the N^1H tautomer **1a** and the N^3H tautomer **1b** can be individually crystallized in the presence of the isocytosinium cation (compound **3**) and neutral 1-methylcytosine (compound **2**). In both compounds, the two partners are involved in formation of three hydrogen bonds.

Applying, in particular, late-transition elements, we have demonstrated in a number of cases that it is possible to isolate and study different metalated forms of tautomers. For example, of the unsubstituted nucleobases cytosine, both N^3 and N^1 linkage isomers of Pt^{II} have been isolated,[27] very much as in the case of uracil anions,[28] and with 1-methylcytosine both metal complexes of the dominant 4-aminooxo tautomer and the rare 4-iminooxo tautomer[29,30] have been crystallized. In one case, even both forms coexist in a single Pt^{II} complex.[31] Similar examples exist for guanine[32] and adenine nucleobases,[33] and the rare 4-hydroxo-2-oxo tautomer of 1-methyluracil has likewise been isolated as a metal-stabilized form.[26a] The topic of metal tautomer complex formation has recently also attracted the interest of theoretical

 © 2005 Wiley-VCH Verlag GmbH & Co. KGaA, Weinheim

and computational chemists,[34–36] who clearly confirm the enormous influence metal coordination can have. Thus in the case of unsubstituted cytosine we detected a remarkable promotion of N^1 binding of am(m)ine-containing Pt^{II} and Pd^{II} species in relationship to the tautomer distribution disfavoring the N^3H tautomer by far.[27] The low abundance of Pt^{II} and Pd^{II} complexes of isocytosine with N^1 coordination[6] in solution and our failure to isolate such compounds, reflect the same principle; unfortunately to our disadvantage. Our efforts to accomplish N^1 coordination of ICH by changing the co-ligands at Pt^{II} to some extent[6] were likewise not successful. These findings are in qualitative agreement with the results of our computational studies which suggest an inherently stronger binding of ICH through N^3 for both Pt^{II} and Pd^{II}.

Experimental Section

Instrumentation: ^{1}H NMR spectra were recorded on Bruker AC200 or Bruker DRX400 instruments in D_2O by using sodium-3-(trimethylsilyl)-propanesulfonate (TSP) as internal reference. Spectra in [D$_6$]DMSO were recorded without presaturation of the water signal using the resonance of [D$_5$]DMSO ($\delta = 2.50$ ppm relative to tetramethylsilane (TMS)) as reference. [D$_6$]DMSO was dried over 4 Å molecular sieves for a week before use or a freshly opened bottle was used. IR spectra (KBr pellets) were recorded on IFS 28 FT spectrometer and Raman spectra on a Coderg T800 with argon (514.5 nm) or krypton laser (647.1 nm) excitation. Elemental analyses were performed with a Carlo Erba Model 1106 Strumentazione elemental analyzer.

pK_a values: pH* values refer to uncorrected pH meter readings (Metrohm 6321; combination glass electrode) in D_2O. pH* values were adjusted by addition of DNO_3 or NaOD solutions; pD values were obtained by adding 0.4 to the uncorrected pH meter reading.

Materials: Isocytosine (ICH) was purchased from Sigma; 9-MeGH and 9-EtGH were obtained from Chemogen (Konstanz, Germany) and guanosine from Sigma-Aldrich. [Pt(dien)I]I,[37] [Pd(dien)I]I,[38] *cis*-[Pt(NH$_3$)$_2$Cl$_2$],[39] and 1-methylcytosine (1-MeC),[40] were prepared according to the methods given in the literature; [Pd(dien)Br]Br was prepared in an analogous manner as [Pd(dien)I]I.[38]

ICH·1-MeC·2H$_2$O (2): 1-MeC (50.0 mg, 0.4 mmol) and ICH (44.4 mg, 0.4 mmol) were dissolved in a minimum amount of water. The solution was warmed at 30 °C till a clear solution was obtained. The solution was concentrated on a water bath and kept for crystallization in air. Colorless crystals appeared after one week. A single crystal was picked and characterized by X-ray crystallography. Elemental analysis calcd (%) for $C_9H_{12}N_6O_2$ (anhydrous sample): C 45.7, H 5.1, N 35.6; found: C 45.5, H 5.0, N 35.2; Raman: $\tilde{\nu} = 1263, 1216, 781, 774, 629$ cm^{-1}.

[1a·ICH$_2$]NO$_3$ (3): ICH (50.0 mg, 0.45 mmol) was dissolved in water and pH of the solution was adjusted to 4.3 with the addition of HNO_3. Colorless crystals were isolated and characterized by X-ray crystallography. Elemental analysis calcd (%) for $C_8H_{11}N_7O_5$ (285.24): C 33.7, H 3.8, N 34.7; found: C 34.0, H 3.8, N 35.0; Raman: $\tilde{\nu} = 1231, 1209, 1046, 1038, 796, 790$ cm^{-1}.

[Pd$_2$(dien)$_2$(IC-N^1,N^3)](ClO$_4$)$_3$ (4): A suspension of [Pd(dien)Br]Br (50.0 mg, 0.135 mmol) in D_2O (1.0 mL) was treated with $AgClO_4$ (55.7 mg, 0.270 mmol) for 5 h at 40 °C with the exclusion of daylight. The solution was then cooled to room temperature, AgBr filtered off, and and the remaining solution was divided into two parts. Isocytosine (7.5 mg, 0.0675 mmol) was added to the first part of the solution. The mixture was again stirred for 5 h at 40 °C. pD of the solution was later adjusted to 7.6 and 150.0 μL of $[Pd(dien)(D_2O)]^{2+}$ solution was added to the mixture. The progress of the reaction was monitored by ^{1}H NMR spectroscopy. This procedure was repeated until only a single set of signals due to [Pd$_2$(dien)$_2$(IC-N^1,N^3)](ClO$_4$)$_3$ was present. Yellow crystals were formed in the reaction mixture within 1 day at 3 °C. Yield 45%. A single crystal was picked and characterized by X-ray crystallography. Elemental analysis calcd (%) for $C_{12}H_{30}N_9O_{13}Pd_2Cl_3$ (827.62): C 17.4, H 3.7, N 15.2; found: C 17.4, H 3.5, N 15.1. Two molecules of water were detected in the X-ray crystal structure. ^{1}H NMR (200 MHz, D_2O, pD = 6.42): $\delta = 7.70$ (d, $J = 7.0$ Hz, 1H; H6), 5.73 (d, $J = 7.0$ Hz, 1H; H5), 3.35, 3.29, 3.12, 3.09, 2.93, 2.90 ppm (m; dien); IR: $\tilde{\nu} = 3400, 3266, 1620, 1563, 1450, 1400, 1300, 840$ cm^{-1}; Raman: $\tilde{\nu} = 1409, 1237, 955, 936, 801, 455$ cm^{-1}.

[Pt$_2$(dien)$_2$(IC-N^1,N^3)](ClO$_4$)$_3$ (5): Compound **5** was obtained in an analogous manner as **4** with [Pt(dien)I]I substituting for [Pd(dien)Br]Br. Colorless crystals formed in the reaction mixture within 2 d at 3 °C, in 25% yield. A single crystal was picked and characterized by X-ray crystallog-

Table 4. Crystallographic data for compounds **2**–**5**.

	2	**3**	**4**	**5**
formula	$C_9H_{16}N_6O_4$	$C_8H_{11}N_7O_5$	$C_{12}H_{34}N_9O_{15}Cl_3Pd_2$	$C_{12}H_{34}N_9O_{15}Cl_3Pt_2$
M_r [g mol^{-1}]	272.28	285.24	863.65	1040.97
habit	blocks	blocks	needles	plates
color	colorless	colorless	yellow	colorless
crystal size [mm]	0.2×0.2×0.1	0.3×0.2×0.2	0.1×0.1×0.4	0.1×0.1×0.3
space group	*C2/c*	*C2/c*	$P2_1/c$	$P2_1/c$
a [Å]	23.541(5)	20.617(5)	14.659(3)	14.598(3)
b [Å]	7.436(2)	5.157 (1)	11.504(2)	11.601(2)
c [Å]	14.529(3)	22.684(4)	21.760(7)	21.769(7)
α [°]	90.00	90.00	90.00	90.00
β [°]	93.88(3)	97.79(3)	129.58 (2)	129.54(2)
γ [°]	90.00	90.00	90.00	90.00
V [Å^3]	2537.5(9)	2389.5(9)	2828.1(14)	2843.0(14)
Z	8	8	4	4
ρ_{calcd} [g cm^{-1}]	1.425	1.586	2.019	2.423
μ [mm^{-1}]	0.114	0.133	1.637	1.109
T [K]	293	293	293	293
F(000)	1152	1184	1712	1968
2θ range [°]	5.6–55.8	5.0–56.6	6.0–55.0	6.6–55.0
index range	$-30 \le h \le 30$	$-26 \le h \le 25$	$-19 \le h \le 19$	$-18 \le h \le 18$
	$-9 \le k \le 0$	$0 \le k \le 6$	$-14 \le k \le 14$	$-15 \le k \le 15$
	$-18 \le l \le 18$	$-29 \le l \le 29$	$-28 \le l \le 28$	$-28 \le l \le 28$
reflns collected	4562	4327	49155	63424
unique reflns[a]	2697	2637	6471	6508
refinement	F_o^2	F_o^2	F_o^2	F_o^2
solution methods	direct	direct	Patterson	Patterson
parameters	236	229	460	460
R_1	0.0335	0.0361	0.0327	0.0306
wR_2	0.0629	0.0818	0.0686	0.0712
R_{int}	0.069	0.043	0.062	0.057
GOF	0.627	0.77	1.15	1.63

[a] With $|F_o| = 4\sigma|F_o|$.

 © 2005 Wiley-VCH Verlag GmbH & Co. KGaA, Weinheim

raphy. Elemental analysis calcd (%) for $C_{12}H_{34}N_9O_{15}Pt_2Cl_3$ (1040.97): C 13.9, H 3.3, N 12.1; found: C 13.7, H 3.2, N 12.1; ^{1}H NMR (200 MHz, D_2O, pD = 6.24): δ = 7.73 (d, J = 7.0 Hz, 1H; H6), 5.77 (d , J = 7.0 Hz, 1H; H5), 3.35, 3.29, 3.12, 3.09, 2.93, 2.90 ppm (m; dien); IR $\tilde{\nu}$ = 3410, 3271, 1633, 1563, 1458, 1409, 1304, 843 cm^{-1}; Raman $\tilde{\nu}$ = 1496, 1409, 1235, 934, 801 cm^{-1}.

[Pt(dien)(ICH-N^1)](ClO$_4$)$_2$ (6): Complex **5** was dissolved in D_2O and the pD of the solution was adjusted to 1.2 by addition of DCl. The progress of the reaction was monitored by ^{1}H NMR spectroscopy. A new set of resonances started to appear immediately after addition of DCl. The solution was then heated at 40 °C for four hours. With time, the signals for the dinuclear complex disappeared and a single set of resonances was present. This set of resonances was assigned to the N^1 linkage isomer on the basis of a pD dependence investigation carried out earlier.[6] Furthermore, Pt satellites are present for the H6 proton of the ICH ligand. Until now, it has not been possible to isolate the compound from solution. ^{1}H NMR (200 MHz, D_2O, pD = 1.41): δ = 7.87 (d, J = 7.6 Hz, 1H; H6), 5.90 (d, J = 7.6 Hz, 1H; H5), 3.35, 3.29, 3.12, 3.09, 2.93, 2.90 ppm (m; dien).

Theoretical calculations: The DFT calculations were performed by using the Gaussian 98 package.[41] A combination of Becke's three-parameter hybrid functional[42] with Lee–Yang–Parr's exchange functional[43] was applied for all structures. The metals in the Pd and Pt complexes have been described with the LANL2DZ basis set, including effective core potentials, while the 6-31G* basis set has been used for C, N, O, and H atoms. The total energy was calculated as the sum of the electronic energy and the zero-point vibrational energy. Vibrational frequency calculations were carried out to ensure that the stationary points located on the potential energy surfaces by geometry optimization were minima.

Crystallographic details: Details of the data collection and refinement of the crystal structures of complexes **2**–**5** can be found in Table 4. Diffraction data for compounds **2**–**5** were collected at room temperature on a Bruker–Nonius Kappa CCD diffractometer[44] using by graphite-monochromated $Mo_{K\alpha}$ radiation (λ = 0.7107 Å) with a sample-to-detector distance of 34 mm and a ω-scan data collection mode with a HKL 2000-Suite program package. Preliminary orientation matrices and unit cell parameters were obtained from peaks of the first ten frames and refined by using the whole data set. Frames were integrated and corrected for Lorentz and polarization effects by using DENZO-SMN.[45] The scaling as well as the global refinement of crystal parameters were performed with SCALEPACK.[45] Reflections, which were partly measured on previous and following frames, were used to scale these frames on each other. Merging of redundant reflections in part eliminates absorption effects and also considers crystal decay if present. The SHELXTL 5.1[46] package was used to solve and refine the structures by direct (**2**, **3**) and Patterson methods (**4**, **5**). Hydrogen atoms were located in a difference Fourier map and refined isotropically while all non-hydrogen atoms were treated anisotropically.

Further details of the crystal structure investigations can be obtained from the Fachinformationszentrum Karlsruhe, 76344 Eggenstein-Leopoldshafen, Germany, (fax: (+49) 7247-808-666; e-mail: crysdata@fiz.karlsruhe.de) on quoting the depository numbers CSD-415499, CSD-415500, CSD-415501 and CSD-415502.

Acknowledgements

This work has been supported by the Deutsche Forschungsgemeinschaft (DFG) and the Fonds der Chemischen Industrie (FCI). Support by the International Max Planck Research School Dortmund/Bochum for D.G. is gratefully acknowledged. We thank Marta Morell Cerdà for her help with X-ray crystallography.

[1] B. D. Sharma, J. F. McConnell, *Acta Crystallogr.* **1965**, *19*, 797–806.
[2] J. F. McConnell, B. D. Sharma, R. E. Marsh, *Nature* **1964**, *203*, 399–400.
[3] J. H Burchenal, K. Ciovacco, K. Kalaher, T. O'Toole, R. Kiefner, M. H. Dowling, C. K. Chu, K. A. Watanabe, J. Fox, *Cancer Res.* **1976**, *36*, 1520–1523.
[4] L. M. Beauchamp, B. L. Serling, J. E. Kelsey, K. K. Biron, P. Collins, J. Selway, J. C. Lin, H. J. Schaeffer, *J. Med. Chem.* **1988**, *31*, 144–149.
[5] A. Ono, P. O. P. Ts'o, L.-s. Kan, *J. Am. Chem. Soc.* **1991**, *113*, 4032–4033.
[6] D. Gupta, M. Huelsekopf, M. M. Cerdà, R. Ludwig, B. Lippert, *Inorg. Chem.* **2004**, *43*, 3386–3393.
[7] W. Brüning, R. K. O. Sigel, E. Freisinger, B. Lippert, *Angew. Chem.* **2001**, *113*, 3497–3500; *Angew. Chem. Int. Ed.* **2001**, *40*, 3397–3399.
[8] C. Hélène, P. Douzou, *C. R. Hebd. Seances Acad. Sci.* **1964**, *259*, 4853–4856.
[9] M. M. Stimson, M. J. O'Donnell, *J. Am. Chem. Soc.* **1952**, *74*, 1805–1808.
[10] H. Morita, S. Nagakura, *Theor. Chim. Acta* **1968**, *11*, 279–295.
[11] J. S. Kwiatkowski, J. Leszczynski, *Int. J. Quantum Chem.* **1997**, *61*, 453–465.
[12] D. J. Brown, T. Teitei, *Aust. J. Chem.* **1965**, *18*, 559–568.
[13] C. Hélène, P. Douzou, *C. R. Hebd. Seances Acad. Sci.* **1964**, *259*, 4387–4390.
[14] T. Chatake, A. Ono, Y. Ueno, A. Matsuda, A. Takénaka, *J. Mol. Biol.* **1999**, *294*, 1215–1222.
[15] T. Chatake, T. Hikima, A. Ono, Y. Ueno, A. Matsuda, A. Takénaka, *J. Mol. Biol.* **1999**, *294*, 1223–1230.
[16] T. W. Bell, Z. Hou, Y. Luo, M. G. B. Drew, E. Chapoteau, B. P. Czech, A. Kumar, *Science* **1995**, *269*, 671–674.
[17] I. Dabkowska, M. Gutowski, J. Rak, *J. Am. Chem. Soc.* **2005**, *127*, 2238–2248.
[18] M. Rossi, T. J. Kistenmacher, *Acta Crystallogr. Sect. B* **1977**, *33*, 3962–3965.
[19] R. Faggiani, B. Lippert, C. J. L. Lock, *Inorg. Chem.* **1982**, *21*, 3210–3216.
[20] R. A. Newmark, C. R. Cantor, *J. Am. Chem. Soc.* **1968**, *90*, 5010–5017.
[21] F. Fujinami, K. Ogawa, Y. Arakawa, S. Shirotake, S. Fujii, K.-I. Tomita, *Acta Crystallogr. Sect. B* **1979**, *35*, 968–970.
[22] a) T. J. Kistenmacher, M. Rossi, C. C. Chiang, J. P. Caradonna, L. G. Marzilli, *Adv. Mol. Relax Interact. Processes* **1980**, *17*, 113–134; b) J. Müller, E. Freisinger, *Acta Crystallogr. Sect. E* **2005**, *6*, o320–o322; c) A. Schimanski, E. Freisinger, A. Erxleben, B. Lippert, *Inorg. Chim. Acta* **1998**, *283*, 223–232.
[23] a) M. C. Wahl, S. T. Rao, M. Sundaralingam, *Nat. Struct. Biol.* **1996**, *3*, 24–31; b) P. Auffinger, S. Louise-May, E. Westhof, *J. Am. Chem. Soc.* **1996**, *118*, 1181–1189; c) G. R. Desiraju, T. Steiner, *The Weak Hydrogen Bond*; Oxford University Press, Oxford, **1999**.
[24] J. F. Britten, C. J. L. Lock, W. M. C. Pratt, *Acta Crystallogr. Sect. B* **1982**, *38*, 2148–2155.
[25] J. F. Britten, C. J. L. Lock, *Acta Crystallogr. Sect. B* **1980**, *36*, 2958–2963.
[26] a) H. Schöllhorn, U. Thewalt, B. Lippert, *J. Am. Chem. Soc.* **1989**, *111*, 7213–7221; b) B. Lippert, *Inorg. Chim. Acta* **1981**, *55*, 5–14; c) H. Schöllhorn, U. Thewalt, B. Lippert, *Inorg. Chim. Acta* **1985**, *106*, 177–180.
[27] a) W. Brüning, E. Freisinger, M. Sabat, R. K. O. Sigel, B. Lippert, *Chem. Eur. J.* **2002**, *8*, 4681–4692; b) W. Brüning, I. Ascaso, E. Freisinger, M. Sabat, B. Lippert, *Inorg. Chim. Acta* **2002**, *339*, 400–410.
[28] H. Rauter, E. C. Hillgeris, A. Erxleben, B. Lippert, *J. Am. Chem. Soc.* **1994**, *116*, 616–624, and references therein.
[29] B. Lippert, H. Schöllhorn, U. Thewalt, *J. Am. Chem. Soc.* **1986**, *108*, 6616–6621.
[30] J. Müller, E. Zangrando, N. Pahlke, E. Freisinger, L. Randaccio, B. Lippert, *Chem. Eur. J.* **1998**, *4*, 397–405.
[31] P. J. Sanz Miguel, P. Lax, M. Willermann, B. Lippert, *Inorg. Chim. Acta* **2004**, *357*, 4552–4561.

 © 2005 Wiley-VCH Verlag GmbH & Co. KGaA, Weinheim

[32] G. Frommer, I. Mutikainen, F. J. Pesch, E. C. Hillgeris, H. Preut, B. Lippert, *Inorg. Chem.* **1992**, *31*, 2429–2434.
[33] a) V. M. Rodriguez- Bailey, M. J. Clark, *Inorg. Chem.* **1997**, *36*, 1611–1618, and references therein; b) J. Arpalahti, K. D. Klika, *Eur. J. Inorg. Chem.* **1999**, 1199–1201; c) J. Viljanen, K. D. Klika, R. Sillanpää, J. Arpalahti, *Inorg. Chem.* **1999**, *38*, 4924–4925; d) M. Garijo Añorbe, M. S. Lüth, M. Roitzsch, M. Morell Cerdà, P. Lax, G. Kampf, H. Sigel, B. Lippert, *Chem. Eur. J.* **2004**, *10*, 1046–1057.
[34] J. V. Burda, J. Šponer, J. Leszczynski, *J. Biol. Inorg. Chem.* **2000**, *5*, 178–188.
[35] A. K. Vrkic, T. Taverner, P. F. James, R. A. J. O'Hair, *Dalton Trans.* **2004**, 197.
[36] D. B. Pedersen, B. Simard, A. Martinez, A. Moussatova, *J. Phys. Chem. A* **2003**, *107*, 6464–6469.
[37] W. A. Cude, G. W. Watt, *Inorg. Chem.* **1968**, *7*, 335–338.
[38] W. H. Baddley, F. Basolo, *J. Am. Chem. Soc.* **1966**, *88*, 2944–2950.
[39] G. B. Kauffman, D. O. Cowan, *Inorg. Synth.* **1963**, *7*, 239–245.
[40] T. J. Kistenmacher, M. Rossi, J. P. Caradonna, L. G. Marzilli, *Adv. Mol. Relax. Interact. Processes* **1979**, *15*, 119–133.
[41] Gaussian 98 (Revision A.7), M. J. Frisch, G. W. Trucks, H. B. Schlegel, G. E. Scuseria, M. A. Robb, J. R. Cheeseman, V. G. Zakrzewski, Jr., J. A. Montgomery, R. E. Stratmann, J. C. Burant, S. Dapprich, J. M. Millam, A. D. Daniels, K. N. Kudin, M. C. Strain, O. Farkas, J. Tomasi, V. Barone, M. Cossi, R. Cammi, B. Mennucci, C. Pomelli, C. Adamo, S. Clifford, J. Ochterski, G. A. Petersson, P. Y. Ayala, Q. Cui, K. Morokuma, D. K. Malick, A. D. Rabuck, K. Raghavachari, J. B. Foresman, J. Cioslowski, J. V. Ortiz, A. G. Baboul, B. B. Stefanov, G. Liu, A. Liashenko, P. Piskorz, I. Komaromi, R. Gomperts, R. L. Martin, D. J. Fox, T. Keith, M. A. Al-Laham, C. Y. Peng, A. Nanayakkara, C. Gonzalez, M. Challacombe, P. M. W. Gill, B. Johnson, W. Chen , M. W. Wong, J. L. Andres, C. Gonzalez, M. HeadGordon, E. S. Replogle, J. A. Pople, Gaussian, Inc., Pittsburgh, **1998**.
[42] A. D. Becke, *J. Chem. Phys.* **1993**, *98*, 5648–5652.
[43] a) C. Lee, W. Yang, R. G. Parr, *Phys. Rev. B* **1998**, *37*, 785–789; b) B. Miehlich, A. Savin, H. Stoll, H. Preuss, *Chem. Phys. Lett.* **1989**, *157*, 200–206.
[44] Bruker-Nonius B. V., Röntgenweg 1, P. O. Box 811, 2600 AV Delft, Netherlands.
[45] Z. Otwinowsky, W. Minor, *Methods Enzymol.* **1997**, *276*, 307–326.
[46] G. M. Sheldrick, SHELXTL-PLUS (VMS), Siemens Analytical X-ray Instruments, Inc. Madison, WI, **1990**; SHELXL-93, Program for crystal structure refinement, University of Göttingen, **1993**; SHELXL-97, Program for the Refinement of Crystal Structures, University of Göttingen, **1997**.

Received: June 16, 2005
Published online: August 25, 2005

 © 2005 Wiley-VCH Verlag GmbH & Co. KGaA, Weinheim